

Syracuse University

**SURFACE**

---

Physics

College of Arts and Sciences

---

2002

## Photocarrier Drift Mobility Measurements and Electron Localization in Nanoporous Silicon

P. N. Rao  
*Syracuse University*

Eric A. Schiff  
*Syracuse University*

L. Tsybeskov  
*University of Rochester*

P. Fauchet  
*University of Rochester*

Follow this and additional works at: <https://surface.syr.edu/phy>

 Part of the [Physics Commons](#)

---

### Recommended Citation

"Photocarrier Drift Mobility Measurements and Electron Localization in Nanoporous Silicon," P. N. Rao, E. A. Schiff, L. Tsybeskov, and P. Fauchet, *Chemical Physics* 284, 129-138 (2002).

This Article is brought to you for free and open access by the College of Arts and Sciences at SURFACE. It has been accepted for inclusion in Physics by an authorized administrator of SURFACE. For more information, please contact [surface@syr.edu](mailto:surface@syr.edu).



# Photocarrier drift-mobility measurements and electron localization in nanoporous silicon

P.N. Rao<sup>a,1</sup>, E.A. Schiff<sup>a,\*</sup>, L. Tsybeskov<sup>b,2</sup>, P. Fauchet<sup>b</sup>

<sup>a</sup> Department of Physics, Syracuse University, Syracuse, NY 13244-1130, USA

<sup>b</sup> Department of Electrical Engineering, University of Rochester, Rochester, NY 14627, USA

Received 1 November 2001

## Abstract

We report photocarrier time-of-flight measurements in diode structures made of highly porous crystalline silicon. The corresponding electron and hole drift mobilities are very small ( $<10^{-4}$  cm<sup>2</sup>/V s) compared to homogeneous crystalline silicon. The mobilities are dispersive (i.e., having a power-law decay with time or length-scale), but are only weakly temperature-dependent. The dispersion parameter lies in the range 0.55–0.65 for both electrons and holes. We conclude that the drift mobilities are limited by the nanoporous geometry, and not by disorder-induced localized states acting as traps. This conclusion is surprising in the context of luminescence models based on radiative recombination of localized excitons.

© 2002 Elsevier Science B.V. All rights reserved.

## 1. Introduction

The opportunities and challenges of disordered, nanostructured materials are very well illustrated by porous silicon samples made by electrochemical etching of single silicon crystals. Porous silicon is a sponge-like network of crystalline silicon twigs and branches. The atoms remaining after etching essentially retain the same positions as in the original crystal, and the finest feature size is on the nanometer scale. As Canham discovered [1] while il-

luminating with ultraviolet light at room temperature, certain porous silicon samples luminesce with an efficiency enormously larger than that for a macroscopic silicon crystal; in addition, there are significant blue-shifts in the optical properties of porous silicon samples compared to those of crystal silicon. Canham's discovery has now generated a sizable literature devoted to understanding this effect and to ideas for exploiting or extending it to create an "all-silicon" opto-electronics [2].

For the most part, an understanding of these properties has been sought from a picture of porous silicon as a loose aggregate of nanocrystals [3]. For example, in one recent experiment [4], porous silicon samples were broken up into pieces estimated to be about 5 nm in size. The photoluminescence spectrum was largely unaffected by this

\* Corresponding author. Fax: +1-315-443-9103.

E-mail address: [schiff@physics.syr.edu](mailto:schiff@physics.syr.edu) (E.A. Schiff).

<sup>1</sup> Present address: Microstrategy, Inc., Fairfax, VA, USA.

<sup>2</sup> Present address: Department of Electrical and Computer Engineering, New Jersey Institute of Technology, Newark, NJ, USA.

process, and the authors concluded that the fundamental size of the light-emitting “chromophore” in porous silicon must be substantially less than 5 nm. It is also well established that both surface passivation conditions as well as the size of the finest feature affect both the magnitude and the spectrum of the luminescence [5,6]. These aspects are fairly consistent with the idea that the luminescence derives from radiative recombination of long-lived excitons localized on individual nanocrystals.

In this paper, we present measurements of the motions of photogenerated electrons and holes as a function of temperature in nanoporous silicon [7]. We deduce photocarrier drift mobilities from these measurements that are enormously ( $\approx 10^7$  times) lower than those for homogeneous crystalline silicon. We also find that the drift mobilities of both electrons and holes are strongly dispersive (i.e., the mobility depends upon the time-scale of the measurement) [8].

Many disordered, but non-porous, photoconductors have drift mobilities with these two features. Most frequently, the features have been explained in terms of a distribution of localized states that “trap” photocarriers, and subsequently release them following a delay characterized by the trap’s binding energy for the carrier. However, the signatures for trapping effects of this type are strong temperature-dependences for the magnitude of the photocarrier drift mobility and for the dispersion parameter. For porous silicon, the temperature-dependence of the drift mobilities that we shall report for both electrons and holes is too weak to be consistent with trapping models. The drift-mobility measurements are consistent with geometrical limitation of transport such as that predicted for transport on a fractal structure; we discuss this approach and its difficulties again at the conclusion of the paper.

The absence or weakness of trapping effects on the photocarrier mobility is probably the most important conclusion we draw from the present work. This conclusion is surprising in the context of the nanocrystal-aggregate model for the luminescence, since each nearly isolated nanocrystal in this model may be considered as a trap for photocarriers. We illustrate some of the concep-

tual issues in Fig. 1, where we have schematically illustrated the electronic density-of-states  $g(E)$  near the bandedge for “macroporous” and for “nanoporous” silicon.

We shall use the idea of a “minimum feature size”  $r_0$  to describe the porosity; we have in mind that  $r_0$  is essentially equivalent to the lower length-scale cutoff invoked in describing fractal struc-

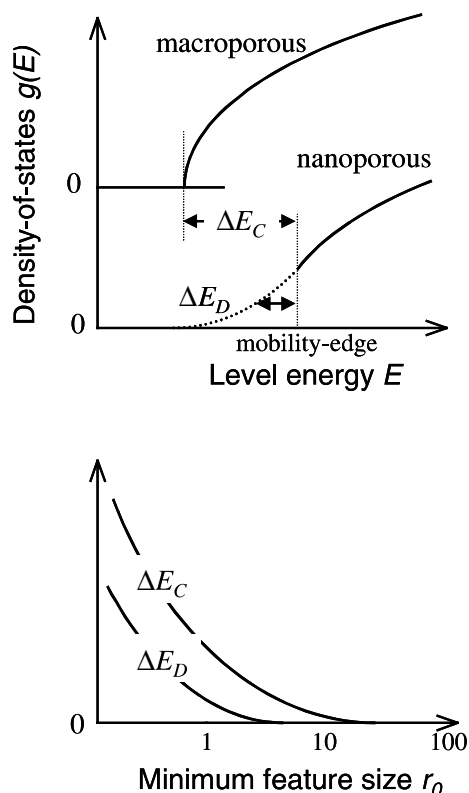


Fig. 1. (upper panel) Electronic density-of-states  $g(E)$  for macroporous silicon (for which the minimum feature size  $r_0$  is tens of nanometers or larger) and for nanoporous silicon (for which the minimum feature size is below 10 nm).  $g(E)$  for macroporous silicon is essentially the same as that for crystal silicon ( $r_0 \rightarrow \infty$ ), and nearly all electronic states are extended. For nanoporous silicon there is a disorder-induced mobility-edge dividing localized and extended electronic states; the localized states form a bandtail of characteristic width  $\Delta E_D$ . There is also a porosity-induced blue-shift  $\Delta E_C$  of the mobility-edge up from the bandedge of the macroporous material. (lower panel) Speculation regarding the dependence of  $\Delta E_C$  and  $\Delta E_D$  upon the minimum feature size  $r_0$  for a disordered porous network; in particular this graph suggests that blue-shifts can remain appreciable in structures with negligible disorder-induced bandtails.

tures. For the  $g(E)$  curve labeled “macroporous” in Fig. 1,  $r_0$  is sufficiently large that porosity has not significantly perturbed the electronic states for crystalline silicon. For the  $g(E)$  curve labeled “nano-porous”,  $r_0$  has nanometer scale, and electronic states are modified through two distinct mechanisms. First, there are porosity-induced blue-shifts  $\Delta E_C$  of the density-of-states. Second, nanoscale disorder is associated with localization. In the figure we show a mobility-edge separating localized and extended states, and we have indicated the width  $\Delta E_D$  of the bandtail of disorder-induced, localized states.

These two effects of nanoporosity are, in principle, independent. Blue-shifts are quite substantial in porous superlattice calculations, which of course have no disorder (and hence no bandtails) [9]. Calculations in the extreme, *quantum percolation* case (atoms randomly occupying lattice sites with densities near the percolation threshold) show very broad bandtails of localized state [10]. In the lower panel of Fig. 1 we show a speculation regarding the dependence of  $\Delta E_C$  and  $\Delta E_D$  upon the minimum feature size of a disordered (nominally a random fractal) porous network; for consistency with the drift-mobility measurements, we have shown the disorder-induced bandtail width  $\Delta E_D$  to be negligible even for regions with significant blue-shifts  $\Delta E_C$ . We return to this speculation and its relationship to luminescence models at the conclusion of the paper.

## 2. Samples

We measured transient photocurrents on two light-emitting, porous silicon (LEPSi) diodes prepared at the University of Rochester; the diodes were prepared independently but with similar procedures. In prior work, these procedures have yielded 0.1% power-efficient, stable light-emitting diodes [11]. Beginning with a p-type Si substrate (resistivity 5–10  $\Omega$  cm), a thin layer (about 0.5  $\mu\text{m}$  thick) is ion-implanted with boron. This structure is then electrochemically etched to yield a two-layer porous structure, viz. a low porosity layer in the ion-implanted region near the top, and a buried, high porosity layer. In one sample this buried

layer was 0.8  $\mu\text{m}$  thick (as ascertained by scanning electron microscopy); in the second it was 1.0  $\mu\text{m}$ . After etching, the structure of the remaining crystalline silicon is essentially undisturbed. Following an oxidation step to passivate the porous layers, the structure is finished by deposition of a polycrystalline,  $n^+$  layer (0.3  $\mu\text{m}$  thick). We made electrical contact to this p–i–n diode using evaporated, semitransparent Al electrodes (area about 0.1  $\text{cm}^2$ ). Using silver paint, we made a simple guard ring around the top Al dot to better define the electrically active region.

The average porosity for the highly porous layer was  $\sim 75$ –80%. The wavelength of the peak intensity for ultraviolet-excited photoluminescence lies between 700 and 750 nm. We crudely estimate that the finest scale of the silicon features is about 3–4 nm from transmission electron micrographs and Raman spectra in comparable samples.

## 3. Transient photocurrent measurements

### 3.1. Technical notes

We obtained estimates of carrier mobilities and other transport parameters from transient photocurrent measurements. Photocarrier pairs consisting of an electron and a hole are generated using laser pulses (3 ns duration) from a nitrogen-pumped dye laser. A voltage bias applied to the material induces photocarrier drift, and we measure the photocurrent transient  $i(t)$  induced by the laser pulse in the bias circuit using a digital oscilloscope. We typically average transient photocurrents from about 100 laser pulses to improve signal–noise ratio. The photocharge transient  $Q(t)$  is calculated by digital integration of  $i(t)$ .

One peculiarity of the present measurements is that we employed DC bias, as opposed to the pulsed bias that is customary in time-of-flight measurements. The reason for this deviation from the standard procedure is the presence of significant dark leakage currents in the structure; the reason for the guard ring noted in the previous section was that these guard rings were fairly effective in reducing the dark currents measured by the bias circuit. However, dark currents in the

range 1–10 mA persisted for bias voltages of  $-10$  V.

With such large dark currents there is no point in using a pulsed bias voltage. The principle of the pulse technique is to guarantee field-uniformity by holding the integrated dark-current below the charge  $CV$  that flows onto the electrodes of the structure immediately following application of the reverse bias voltage. For larger dark currents, this method is useless, and in fact we were unable to obtain interpretable transients using pulsed bias.

We believe that the fields across the high-porosity silicon of our structures were essentially uniform under our measurement conditions [7]. We estimated the “stored charge” of our diodes under our measurement conditions by measuring the time-integrated “recovery current” when bias voltage was removed; we found that this recovery charge was smaller than  $CV$ , in agreement with the assumption of near-uniformity. As we show subsequently, the transient photocurrents were also reasonably consistent with the assumption of uniformity.

### 3.2. Transient measurements

In Fig. 2 we show the photocharge  $Q(t)$  and the photocurrent  $i(t)$  measured in the  $1.0 \mu\text{m}$  sample at  $250$  K for three reverse bias voltages  $V$ . The laser wavelength was  $445$  nm, which is strongly absorbed by the topmost silicon layers and by the highly porous silicon. We do not expect carriers generated in the topmost layers to contribute much to the observed photocurrent, since there is little electric field in these conductive layers. Holes generated in the highly porous layer are swept by the field towards the substrate, and are expected to dominate the photocurrents and photocharges.

The photocharge  $Q(t)$  rises as a power-law and reaches a plateau near  $10^{-4}$  s (depending on the voltage). We shall refer to the value of  $Q(t)$  in this plateau as the total photocharge  $Q_0$ ; when sufficient time has elapsed, all of the holes should have traversed the high-porosity layer. Ideally,  $Q_0$  should be independent of voltage; the increase in  $Q_0$  with  $V$  is probably due to increased “bleeding” of charge out of the low-porosity layer as it is depleted by increasing reverse bias. Examining the

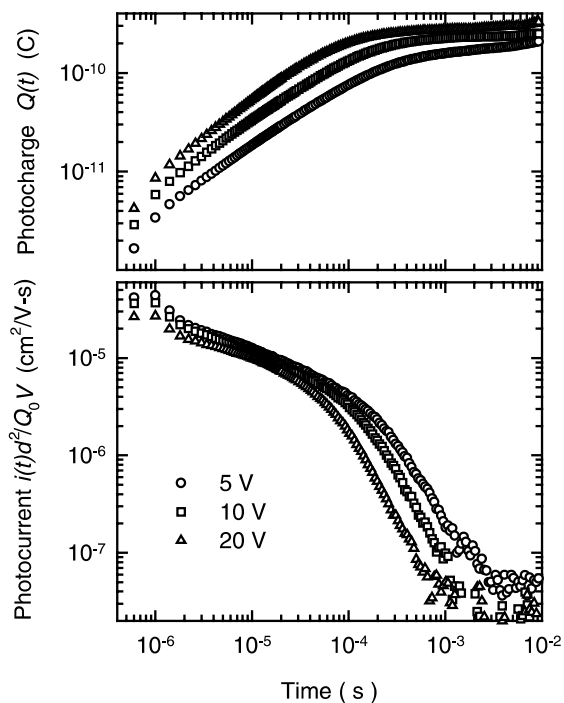


Fig. 2. Transient photocharge and photocurrent measurements at  $250$  K in a porous silicon based light-emitting diode ( $1.0 \mu\text{m}$  thickness of high-porosity layer). Measurements were done following absorption of a  $3$  ns,  $445$  nm pulse from a laser. Results at three bias voltages are shown. Note the constancy of the final charge (upper panel), the decrease in the “transit time” as the reverse bias increases (lower panel), and the power-law (“dispersive”) decay of the photocurrent prior to the transit time.

lower panel of the figure, we further note that the photocurrent is linear with bias voltage for earlier times. The  $5$  V transient establishes an envelope for  $i(t)/V$  from which higher voltage transients break away at increasingly earlier “transit times”  $t_T$ . For later reference, we note that we note that this typical “transit time” is essentially the time required for the photocharge to reach half its terminal value  $Q_0/2$ . We have multiplied the photocurrent  $i(t)/V$  by the factor  $d^2/Q_0$ , where  $d$  is the thickness of the high-porosity layer. This multiplication converts  $i(t)/V$  to mobility units ( $\text{cm}^2/\text{V s}$ ), and the vertical axis indicates the range of mobilities associated with the hole motion.

In Fig. 3 we illustrate the behavior of the photocharge transients with temperature  $T$  at constant bias voltage  $10$  V. It may be noted that the “transit time” decreases modestly with in-

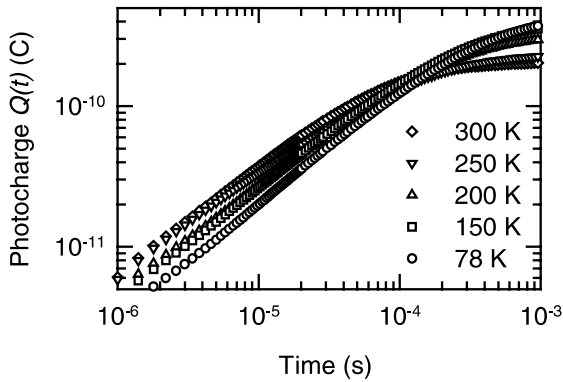


Fig. 3. Transient photocharge measurements in a p-Si diode (1.0  $\mu\text{m}$ ) at 10 V reverse bias and several temperatures. Note the weak temperature-dependence of the measurements.

creasing temperature; we discuss this dependence at length subsequently. In addition,  $Q_0$  increases with falling temperature. This behavior is consistent with an *increasing* bandgap of the top layers as the temperature falls; as these layers become more transparent, the photocharge absorbed in the high-porosity layer increases.

In Fig. 4 we present photocurrent and photocharge transients at 125 K in the second sample (0.8  $\mu\text{m}$ ) using 445 nm laser pulses. The measurements were done with somewhat lower pulse intensities and voltages than for Figs. 2 and 3. They exhibit carrier sweepout effects less perfectly than for the previous data, but appear consistent with the same interpretation.

In Fig. 5 we present the photocharge and photocurrent measured in the 0.8  $\mu\text{m}$  sample, but using a significantly longer wavelength 670 nm. As a consequence of the longer wavelength, most carriers will be absorbed much more deeply in the structure. We believe that most absorption actually occurs in the underlying p-type c-Si substrate. As is evident in Fig. 5, the behavior of the photocharge and photocurrent transients exhibit photocarrier sweepout behavior comparable to that found at 445 nm. We believe that these effects are now due to photocarriers generated in the substrate. The electron photocarriers diffuse into a depletion layer near the boundary with the porous material, and subsequently drift across high-porosity layer. Some evidence for this model can be adduced from the early time form for the transient

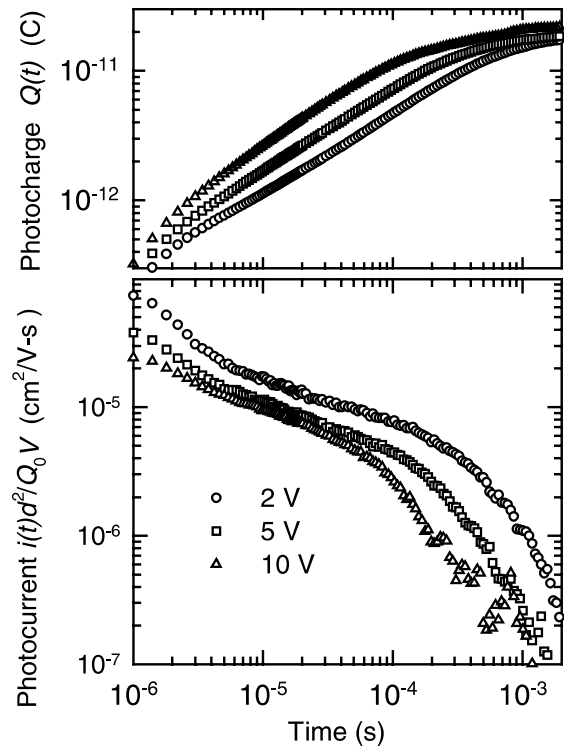


Fig. 4. Transient photocharge and photocurrent measurements at 125 K in a porous silicon based light-emitting diode (0.8  $\mu\text{m}$ ). Measurements were done following absorption of a 3 ns, 445 nm pulse from a laser; results at three bias voltages are shown.

photocharge in Fig. 5, which indicates a “prompt” photocharge collection of about 10% of  $Q_0$  at  $-10$  V prior to the “sweepout” regime. We speculatively attribute this component of the photocharge to motion of the electrons across a depletion zone; a rough calculation indicates that the prompt photocharge is of the correct magnitude. Finally, in Fig. 6 we illustrate the temperature-dependence of the photocharge for 670 nm illumination. Note that  $Q_0$  is less temperature-dependent than for the 445 nm transients.

### 3.3. Drift mobilities and dispersion parameters

Most of the effects present in the measurements summarized in Figs. 2–6 appear consistent with “time-of-flight” effects in a system where drift velocities are linear with electric field, and in this section we present the corresponding analysis in

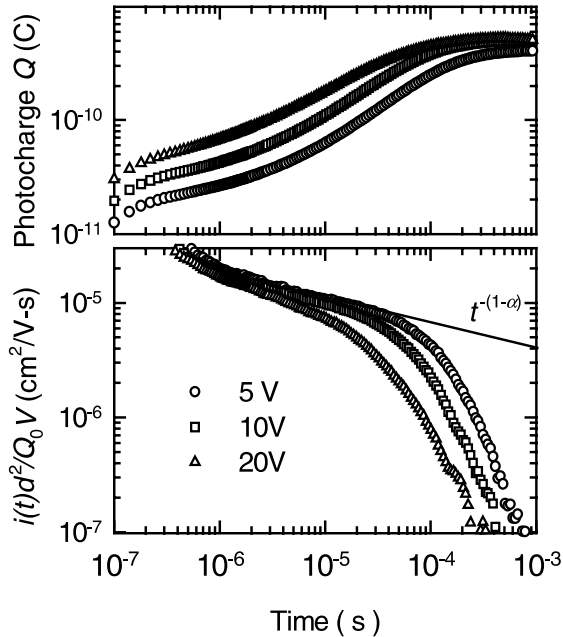


Fig. 5. Transient photocharge and photocurrent measurements at 200 K in a porous silicon based light-emitting diode (0.8  $\mu\text{m}$ ). Measurements were done following absorption of a 3 ns, 670 nm pulse from a laser. Results at three different reverse bias voltages are shown.

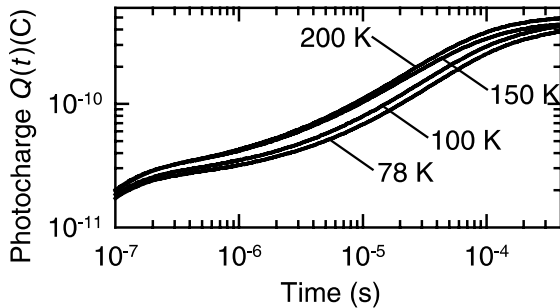


Fig. 6. Transient photocharge measurements in p-Si diode (0.8  $\mu\text{m}$ ) at 10 V reverse bias and several temperatures.

terms of mobilities. One indication of the corresponding carrier drift mobility can be obtained from the vertical scale  $i(t)d^2/Q_0V$  of the photocurrent plots: a mobility of  $10^{-5} \text{ cm}^2/\text{V s}$  characterizes transport about 1  $\mu\text{s}$  following photo-generation of the carriers, where we take  $d$  as the thickness of the highly-porous, middle layer of the light-emitting diodes.

We draw attention to the power-law decay of the photocurrent  $i(t) \propto t^{-(1-\alpha)}$ , which is indicated by the solid line in the photocurrent graph in Fig. 5. The mobility estimated from the pre-transit value of  $i(t)$  is thus time-dependent. Photocurrent drift in systems with such a power-law decay of the photocurrent is denoted as “dispersive”, with  $\alpha$  being the *dispersion parameter*. Many disordered systems exhibit dispersive transport [8]. Single crystals more typically exhibit “Gaussian” transport, where one considers the mobility as time-independent.

It is customary to analyze dispersive drift using a conventional drift mobility derived from the transit times  $t_T$  using the expression  $\mu_D \equiv (L/Et_T)$ , where  $L$  is the displacement of the photocarriers from their initial positions at the time  $t_T$ , and  $E$  is the electric field. We use this mobility definition, which depends upon  $L/E$ , subsequently. Transit times observed in the figures presented above correspond to  $L/E = d^2/2V$ , where  $d$  is the thickness of the high-porosity layer and  $V$  is the bias voltage.

In the upper panel of Fig. 7, we present the temperature-dependence of the conventional drift mobilities  $\mu_D$  for  $L/E = 1 \times 10^{-9} \text{ cm}^2/\text{V}$ . The measurements identified as “holes” were performed using 445 nm laser pulses; measurements identified as electrons were done using 670 nm laser pulses. The lower panel indicates the temperature-dependence of the dispersion parameter. In both these panels, we have used dark solid lines to show literature values of  $\mu_D$  and  $\alpha$  for holes in hydrogenated amorphous silicon (a-Si:H) [12].

## 4. Discussion

### 4.1. Comparison with previous measurements

We briefly discuss prior mobility experiments on porous silicon [13]. The earliest work on photocurrent transients in porous silicon did not yield drift-mobility estimates [14]. The magnitude of the drift mobility and observation of dispersion in the present measurements are broadly consistent with electroluminescence modulation [15] and

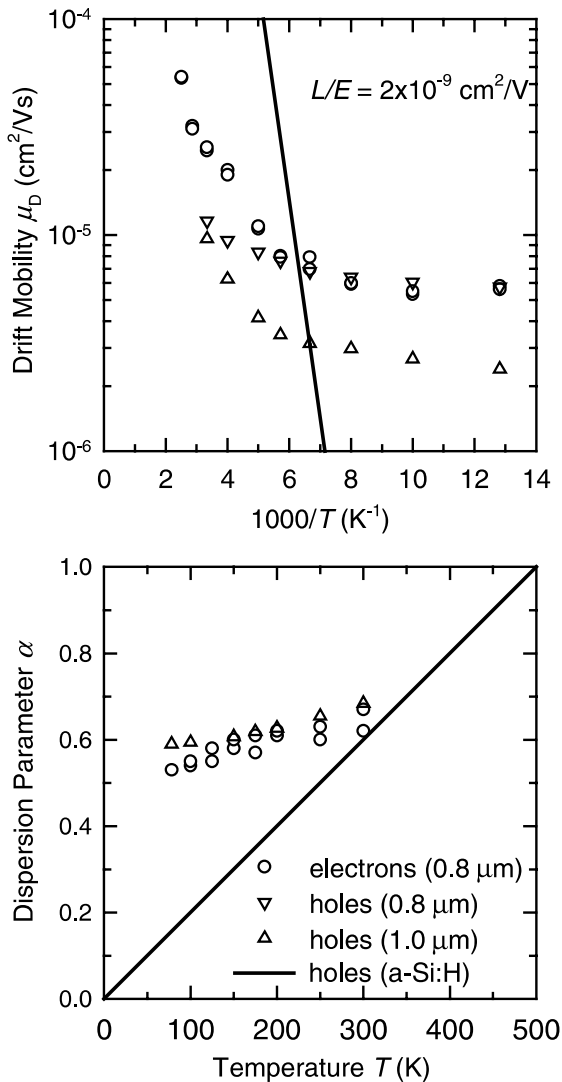


Fig. 7. Temperature-dependence of the magnitude and dispersion of the drift-mobilities measured in two porous-silicon based light-emitting diode. The bold continuous lines indicate measurements for holes in hydrogenated amorphous silicon [12]. The magnitudes correspond to a specific ratio  $L/E = 2 \times 10^{-9} \text{ cm}^2/\text{V}$  of the carrier displacement  $L$  to the electric field  $E$ .

independent time-of-flight measurements [16]. We are not aware of temperature-dependent drift-mobility measurements prior to our own.

At first glance, the very small values we measure of the drift mobilities are not surprising. Small drift mobilities are self-consistent with the porous

structure, since electrochemical etching preferentially attacks relatively homogeneous regions with a higher mobility. Additionally, the drift-mobility near room-temperature is comparable to that for holes in a-Si:H, a second form of disordered silicon. For a-Si:H, the low mobility is primarily a consequence of disorder-induced, localized states near the band edges, and it would not be surprising to find similar effects in porous silicon. Localized states act as “traps” that capture and immobilize carriers until they can be thermally re-emitted into more extended “transport states” at or above the *mobility edge*, which divides localized and extended states. For several amorphous semiconductors, an exponential bandtail *multiple-trapping* model offers a satisfactory explanation for the dispersion parameter and magnitude of the drift mobility [17].

#### 4.2. Absence of trapping effects and luminescence measurements

It is the measurements of weak temperature-dependences for the drift mobility and for the dispersion parameter in porous silicon that are surprising in the context of previous measurements in disordered semiconductors. As illustrated in Fig. 7, dispersive mobility measurements in amorphous semiconductors are associated with a strong temperature-dependence that is absent in the porous silicon measurements. Additional evidence for this experimental conclusion about porous silicon can be inferred from modeling of resonant photoluminescence measurements [18], which concluded that transport was temperature-independent and hence not responsible for the stronger temperature-dependence of luminescence. Despite the common presence of disorder and dispersion in porous and non-crystalline silicon, and despite our expectations that the structure of porous silicon might confine its electronic states, we infer that the measured drift mobilities in porous silicon are not a consequence of multiple trapping by localized states.

An alternative explanation for a weak temperature-dependence is that it results from cancellation of two effects on mobility. The trapping effect leads to reduced mobility as temperature declines,



since carriers are immobilized for increasingly long times on a given trap. However, the fundamental (or “microscopic”) mobility that describes drift of a carrier while it is mobile and untrapped may exhibit the reverse effect; the microscopic mobility may increase as the temperature is reduced because of a corresponding reduction in thermal disorder. For example, the phase coherence length for electrons that is inferred in measurements of thin metal wires increases as temperature declines [19,20].

We do not favor this “cancellation” viewpoint because it requires an apparently accidental congruence of two effects over a broad range of temperature, but it is worth noting that this type of temperature effect cannot be excluded for porous silicons.

The conclusion that trapping is negligible has important implications for modeling of luminescence of porous Si. The relatively large luminescence efficiency, which precipitated much of the last decade’s work on this material, has often been interpreted phenomenologically in terms of a nanocrystal aggregate model [5,6,21]. This model assumes full, three-dimensional confinement of carriers in nanocrystals, which would then effectively be traps.

It is worth noting that the substantial blue-shifts in optical properties for porous silicon (relative to single-crystal silicon) do not imply significant localization, since such blue-shifts may be a global effect of nanoporosity [9]. However, the recent evidence from single-molecule spectroscopy that the structures (or “chromophores”) responsible for photoluminescence in p-Si are very small (<5 nm) seems conclusive. There is thus an apparent contradiction between the absence of trapping effects in transport and the presence of 5 nm chromophores for photoluminescence. We therefore speculate that excitons, which also seem to be conclusively involved in luminescence [22], are more readily localized in porous silicons than are individual electrons and holes. This speculation may also apply to the quenching of photoluminescence in porous silicon diodes under voltage bias [23]; we envisage that the voltage bias might break up bound excitons into independent electrons and holes.

### 4.3. Semiclassical transport on a fractal

We now turn to the broader implications of our work for understanding the effects of disorder on transport. It is apparent that the results of quantum percolation models do not describe our measurements; these calculations predict bandtails of localized states similar to those encountered in amorphous semiconductors. This inapplicability is not a complete surprise, since the minimum feature size in porous silicons is much larger than the atomic scale involved in quantum percolation. The other extreme for modeling transport on a disordered porous matrix is a random walk on a *random fractal* structure [24]. As we discuss shortly, this model should not be directly applicable to our experiment – but we describe it anyway since it provides a satisfactory, phenomenological description of the data.

The diffusion of a particle is conventionally expressed in the form [25,26]  $\langle r^2(t) \rangle \propto t^{2/d_w}$ , where  $\langle r^2 \rangle$  is the mean-square displacement of the particle from its origin at  $t = 0$  and  $d_w$  is the “random walk” dimension. For homogeneous materials,  $d_w = 2$ ; for a fractal, the expression  $d_w = (2d_F/d_S)$  obtains [27,28], where  $d_F$  is the mass dimensionality of the fractal (describing the scaling of the mass inside spheres of different radii viz.  $m \propto R^d$ ), and  $d_S$  is the “spectral” or “fracton” dimensionality characterizing the branching of the fractal. Assuming validity of a generalized Einstein relation [29,30], we may tentatively identify the ratio  $2/d_w$  with the dispersion parameter  $\alpha$  extracted from the drift-mobility data.

Since  $d_w$  is a purely geometrical property of the porous structure, these fractal effects do not lead to any temperature-dependence of diffusion or dispersion. The model is thus reasonably consistent with the measurements presented above. For a dispersion parameter  $\alpha \approx 0.6$ , we obtain  $d_w = 3.3$ . This value for  $d_w$  is similar to estimates for classical percolation networks in three dimensions [25].

Random-walk dimensions have also been estimated for porous silicon samples from DC and AC transport measurements [31,32]. Ben-Chorin et al. [32] estimate  $d_w = 4$  from the frequency dependent AC conductivity of an unilluminated sample with 50–60% porosity. Both the random-walk dimen-

sion, and the weak temperature-dependence of the AC conductivity at frequencies above 1 kHz, are similar to the behavior of the mobilities inferred in the present work from photocarrier behavior. Ben-Chorin et al. propose that their measurements, which are conducted in the dark, are sensitive to electrons occupying traps with a nearly uniform level distribution near the Fermi energy.

While the similarities in the photocarrier transient and AC conductivity measurements do suggest that the fundamental transport physics of the two experiments should also be similar, for the present work we prefer an interpretation in terms of electron levels near a mobility-edge instead of near the Fermi energy. The preference is based on the absence of any experimental signature in our transient measurements for complete photocarrier thermalization (down to the Fermi energy). However, we have little insight into the negligibility of electron traps just below the mobility-edge; a deeper understanding appears to require a theory that better addresses those porous materials where disorder is “cut-off” at the nanometer scale. Moreover, semiclassical transport on a fractal – from which we have drawn an explanation for temperature-independent dispersion – does not directly apply to motions on length scales less than about 20 nm, where quantum size effects must be considered. Inferences about the actual structure of porous silicon (e.g., mass or fracton dimensions) based on the random-walk dimension  $d_w$  are most likely premature.

### Acknowledgements

The authors thank Qing Gu for his measurements on drift mobilities in porous silicon, and thank Shantenu Jha and Cristina Marchetti for discussions. A referee suggested the discussion of quantum transport effects. Research at University of Rochester was partially supported by the Army Research Office.

### References

- [1] L.T. Canham, *Appl. Phys. Lett.* 57 (1990) 1046.
- [2] D.J. Lockwood (Ed.), *Light Emission in Silicon: From Physics to Devices*, Vol. 49 of *Semiconductors and Semimetals*, Academic Press, New York, pp. 206–252.
- [3] L. Brus, *J. Phys. Chem.* 98 (1994) 3575.
- [4] M.D. Mason, D.J. Sirbully, P.J. Carson, S.K. Buratto, *J. Chem. Phys.* 114 (2001) 8119.
- [5] M.V. Wolkin, J. Jorne, P.M. Fauchet, G. Allan, C. Delerue, *Phys. Rev. Lett.* 82 (1999) 197.
- [6] X.J. Li, Y.H. Zhang, *Phys. Rev. B* 61 (2000) 12605.
- [7] A preliminary account of the present work has been given earlier: P.N. Rao, E.A. Schiff, L. Tsybeskov, P.M. Fauchet, in: R.W. Collins (Ed.), *Advances in Microcrystalline and Nanocrystalline Semiconductors-1996*, Symposium Proceedings, vol. 452, Materials Research Society, Pittsburgh, 1997, p. 613.
- [8] H. Scher, M.F. Schlesinger, J.T. Bendler, *Phys. Today* 44 (1) (1991) 26.
- [9] M. Cruz, C. Wang, M.R. Beltran, J. Taguena-Martinez, *Phys. Rev. B* 53 (1996) 3827.
- [10] C. Soukoulis, Q. Li, G.S. Grest, *Phys. Rev. B* 45 (1992) 7724; A. Aharony, O. Entin-Wohlman, A. Brooks Harris, *Physica A* 200 (1993) 171; R. Berkovits, Yshai Avishai, *Phys. Rev. B* 53 (1996) R16125, are some of the references.
- [11] L. Tsybeskov, S.P. Duttagupta, K.D. Hirschman, P.M. Fauchet, in: D.J. Lockwood, P.M. Fauchet, N. Koshida, S.R.J. Burek (Eds.), *Advanced Luminescent Materials*, The Electrochemical Society, Pennington, 1996, p. 34.
- [12] Q. Gu, C. Wang, E.A. Schiff, Y.-M. Li, C.T. Malone, *J. Appl. Phys.* 76 (1994) 2310.
- [13] A.J. Simons, in: L. Canham (Ed.), *Properties of Porous Silicon*, INSPEC, London, 1998, p. 176.
- [14] A. Fejfar, I. Pelant, E. Sipek, J. Kocka, G. Juska, T. Matsumoto, Y. Kanemitsu, *Appl. Phys. Lett.* 66 (1995) 1098, and references therein.
- [15] C. Peng, P.M. Fauchet, *Appl. Phys. Lett.* 67 (1995) 2515.
- [16] E.A. Lebedev, E.A. Smorgonskaya, G. Polisski, *Phys. Rev. B* 57 (1998) 14607.
- [17] T. Tiedje, B. Abeles, J.M. Cebulka, *Solid State Comm.* 47 (1983) 493, is representative; there are many papers on drift mobilities in amorphous silicon and related materials.
- [18] I. Mihalcescu, J.C. Vial, R. Romestain, *Phys. Rev. Lett.* 80 (1998) 3392.
- [19] D. Hoadley, P. McConville, N.O. Birge, *Phys. Rev. B* 60 (1999) 5617.
- [20] S. Friedrichowski, G. Dumpich, *Phys. Rev. B* 58 (1998) 9689.
- [21] C. Delerue, G. Allan, M. Lannoo, in: D.J. Lockwood (Ed.), *Light Emission in Silicon: From Physics to Devices*, Vol. 49 of *Semiconductors and Semimetals*, Academic, New York, 1998, p. 253 (recent review).
- [22] J. Diener, D. Kovalev, H. Heckler, G. Polisski, F. Koch, *Phys. Rev. B* 63 (2001) 73302.

- [23] M. Parkinson, S.C. Bayliss, D.T. Clarke, D. Law, G. Beamson, *Thin Solid Films* 326 (1998) 194.
- [24] B.B. Mandelbrot, *The Fractal Geometry of Nature*, Freeman, San Francisco, 1983.
- [25] Y. Gefen, A. Aharony, S. Alexander, *Phys. Rev. Lett.* 50 (1983) 77.
- [26] T. Nakayama, K. Yakubo, R. Orbach, *Rev. Mod. Phys.* 66 (1994) 381.
- [27] S. Alexander, R. Orbach, *J. Phys. (Paris) Lett.* 43 (1982) L-625.
- [28] R. Rammal, G. Toulouse, *J. Phys. (Paris) Lett.* 44 (1983) L13.
- [29] J.P. Bouchaud, A. Georges, *Phys. Rep.* 195 (1990) 127.
- [30] Q. Gu, E.A. Schiff, S. Grebner, F. Wang, R. Schwarz, *Phys. Rev. Lett.* 76 (1996) 3196.
- [31] A.I. Yakimov, N.P. Stepina, A.V. Dvurechenskii, L.A. Shcherbakova, *JETP* 85 (1997) 501.
- [32] M. Ben-Chorin, F. Moller, F. Koch, W. Schirmacher, W.M. Eberhard, *Phys. Rev. B* 51 (1995) 2199.